Electronic structure and microwave dielectric properties of Al and N co-doped 3C-SiC

ZHIMIN LI*, ZI YANG, CHUANGCHUANG HE, MAOLIN ZHANG, YUNXIA HUANG, YUE HAO
School of Advanced Materials and Nanotechnology, Xidian University, Xi'an 710071, China

The formation energy, electronic structure and complex permittivities of 3C-SiC with different Al and N codoping levels were studied by the first principles plane wave pseudo-potential method based on the density functional theory. Results showed that the incorporation of N into SiC lowered the formation energy of Al-doped SiC, and that the band gap of co-doped SiC increased with increasing Al level. Both real part ε′ and imaginary part ε″ of complex permittivities for co-doped SiC in the frequency range of 8.2-18GHz increased firstly, and then decreased as the level of Al increased, with the maximum values in ε′ and ε″ for Al_3-N complex.

(Received June 11, 2014; accepted October 28, 2015)

Keywords: 3C-SiC, Codoping, Electronic structure, Dielectric property

1. Introduction

In recent years, the microwave absorbers in GHz frequency range have been paid much attention for their extensive use in commercial and military applications [1-3]. Silicon carbide (SiC) has excellent properties, e.g. high strength and hardness, good corrosion resistance, and high thermal stability and thermal conductivity [4, 5], which makes SiC a potential candidate for microwave absorbing materials used at higher temperature. It had been reported that the microwave dielectric properties of SiC at X band could be improved through n- or p-type doping, and the dielectric properties of SiC absorbers were closely relevant with the doping level of dopants [6, 7]. However, for p-type doped SiC absorber with Al, there exists the limitation of Al doping solubility which hinders the further improvement of microwave dielectric properties.

Yamamoto and Yashida [8] investigated the electronic structure of ZnO and found that the concentration of acceptor N could be increased by Al and N codoping approach. Wu et al. also reported that the doping concentration of Mg for AlN was enhanced through Mg:O codoping [9]. Additionally, the electrical property of SiC nanotubes had been adjusted by the means of N and B codoping [10]. Hence, it is possible that the limitation of Al doping concentration may be broken through the Al and N codoping approach for Al-doped SiC microwave absorber, to improve its microwave dielectric property. In this study, the formation energy, electronic structure and complex permittivities of Al and N co-doped 3C-SiC were studied by the first principles plane wave pseudo-potential method based on the density functional theory, and the mechanism of microwave loss for SiC by Al and N codoping was discussed.

2. Methods

In this study, the SiC model was cubic 3C-SiC with zinc blend structure and space group of $F\bar{4}3m$, in which each Si or C atom adjoined with four other species by covalent bonds. The lattice parameters of SiC are a=b=c=0.4358 nm and $\alpha=\beta=\gamma=90^o$. The supercell with 64 atoms was employed by a 2×2×2 replication from the conventional 8 atoms cubic unit cell of 3C-SiC, as shown in Fig. 1. In the supercell, one C atom was replaced by N atom at the center of the cubic, while Al atoms occupied the nearest Si sites to form Al–N codoping complexes [11]. The structural optimization was carried out before the formation energy, electronic structure and permittivities were calculated for Al and N co-doped SiC.

The calculations were carried out using first-principles plane wave pseudo-potential method based on the density functional theory, with Cambridge Serial Total Energy Package(CASTEP) code. The generalized gradient approximation (GGA) was employed with Perdew-Burke-Emzerhof (PBE) to deal with exchange correlation function. The electronic wave function was unfolded with plane wave base groups, and the interaction potentials among ion core and valence electron were represented by ultrasoft pseudo-potential [12, 13]. The valence electron configurations for Si, C, Al and N were $3S^23P^2$, $2S^22P^2$, $3S^23P^1$ and $2s^22p^3$, respectively. The computational accuracy was controlled by selecting appropriate kinetic cutoff energy in reciprocal space. In this study, the plane wave cutoff energy was set to be

380eV, and special K points of 3×3×3 under the Monkhorst-Pack scheme was employed. The self-consistent filed (SCF) tolerance was 1.0×10^{-6}eV/atom.

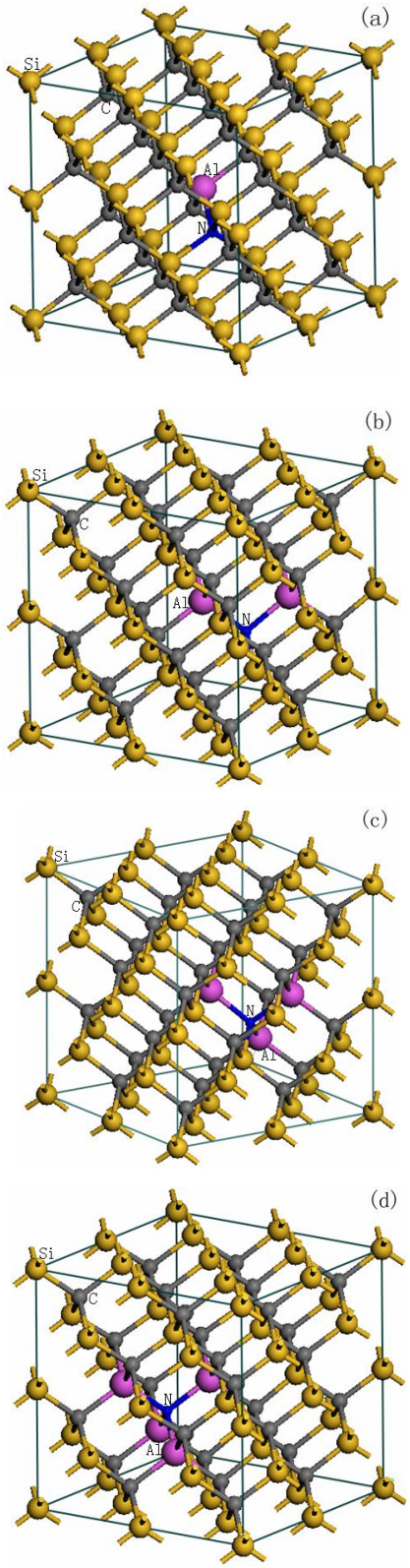

Fig. 1. (2×2×2) supercell of Al and N co-doped 3C-SiC: (a) Al-N; (b) Al_2-N; (c) Al_3-N; (d) Al_4-N

3. Results and discussion

3.1 Structural stability of co-doped 3C-SiC

To study the structural stability of the co-doped 3C-SiC with Al and N, we had calculated the defect formation energy compared to the intrinsic SiC by the following Eq.(1) [10]:

$$E_{form}=E_{tot}(doped)+E(doped)-E_{tot}(intrinsic)-E(doping) \quad (1)$$

Where E_{form} is the defect formation energy of co-doped SiC, E_{tot}(doped) and E_{tot}(intrinsic) are the total energy of co-doped and intrinsic SiC in a supercell, respectively, E(doped) is the energy of carbon or silicon atoms doped by N or Al atoms, respectively, and E(doping) is the energy of free doping N or Al atoms.

Table 1. Defect formation energies (E_{form}) and band gaps (E_g) of 3C-SiC with different Al-N complexes

Complexes	Al-N	Al_2-N	Al_3-N	Al_4-N	Al_2
E_{form}/eV	-1.423	-0.109	1.399	3.059	3.627
E_g/eV	1.292	1.349	1.415	1.445	1.394

The formation energies of SiC doped with Al-N complexes are listed in Table 1. It is well-known that the lower formation energy E_{form} indicates a more stable structure. As can be seen, the formation energy of the system with single Al and N atom co-doping is -1.423eV. This minimum value in all doped complexes was possibly due to the annihilation of the electron and hole arising from N and Al doped atom, respectively [14]. Although the formation energy increased with increasing Al atoms, all the E_{form} of Al and N co-doped SiC in table.1 were less than that of SiC containing two Al atoms. Obviously, the incorporation of N into SiC structure decreased the formation energy of the system only doped with Al.

3.2 Band structures and density of states

The band structures of Al and N co-doped SiC calculated from the high symmetry points of brillouin zone are showed in Fig. 2. It can be found that all the Fermi levels for doped SiC enter the valence band, indicating the characteristic of p-type doping [15], and that the band gap of the co-doped SiC becomes greater as the Al doped atom increases, as showed in the Table 1. Additionally, an increase in energy levels for doped SiC will contribute to the increase of electrical conductivity of the material.

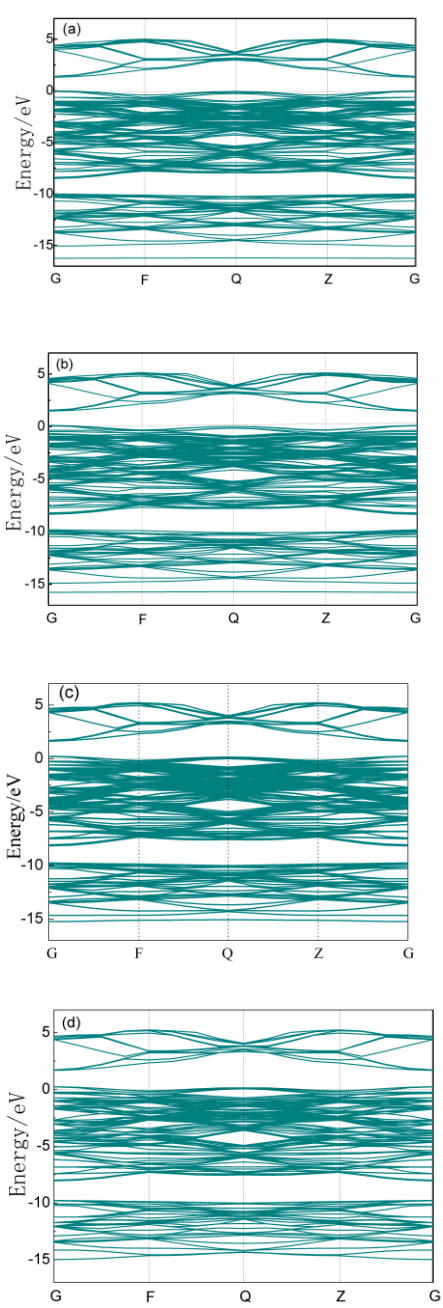

Fig. 2. Band structures of Al and N co-doped 3C-SiC: (a) Al-N; (b) Al_2-N; (c) Al_3-N; (d) Al_4-N

Fig. 3 shows the density of states (DOS) and partial density of states (PDOS) of Al-N, Al_2-N, Al_3-N and Al_4-N co-doped 3C-SiC. It can be seen that the valence bands of the co-doped 3C-SiC consist of two parts, in agreement with the results of Fig. 2. The lower valence band (-15eV—-10eV) was formed mainly by Si 3s3p、N 2s and C 2s states, and the upper valence band (-8.2eV—0eV) was ascribed to Si 3p, Al 3p, N 2p and C 2p states. Especially, Al 3p and C 2p states contributed to the valence band top close to the Fermi level, which was relevant with the character of material. As a result, Al doping increased the DOS near Fermi level, as well as the density of the carrier that was available on the electrical conductivity and permittivity of SiC. Furthermore, the top of valence band of co-doped SiC shifted to the direction of higher energy with the increasing Al levels. It was because that Al doping formed impurity level that would repel the electron on the valence band top towards the lower energy, and that hole carrier derived from transition distributed on the impurity level, leading to broaden density of states [16]. While the conduction band was composed of the states of Si 3p and Al 3p, which also moved towards the higher energy with the increasing Al atoms, resulting in the broader band gap of SiC.

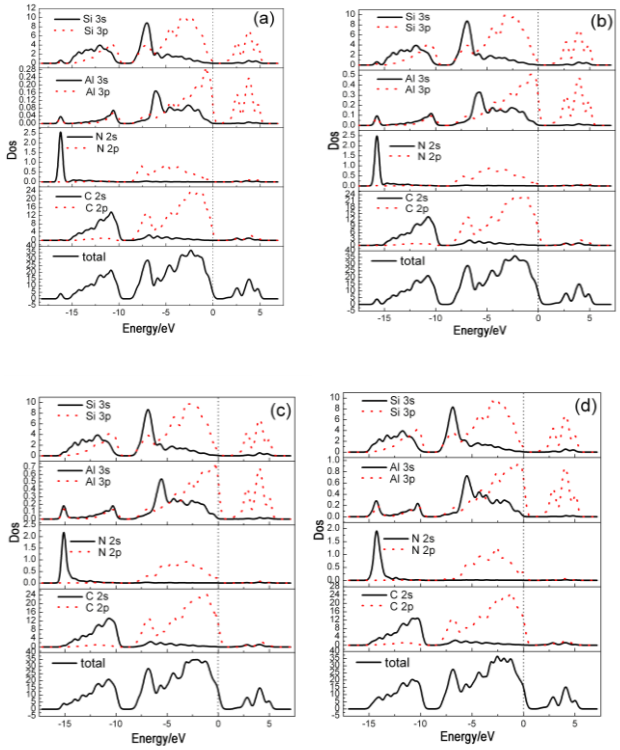

Fig. 3. Total density of states (DOS) and partial density of states PDOS of co-doped 3C-SiC: (a) Al-N; (b) Al_2-N; (c) Al_3-N; (d) Al_4-N

3.3 Dielectric properties

For SiC microwave absorber, considering the applied frequency range of 8.2-18GHz which corresponds to the energy range of 3.39×10^{-5}-7.45×10^{-5} eV, we calculated the real part ε′ and imaginary part ε″ of permittivities of co-doped 3C-SiC in the energy range of 0-2eV, as shown in Fig. 4. It can be seen that the ε′ and ε″ for all the co-doped 3C-SiC have a significant variation in lower energy region. Both the real part ε′ and imaginary part ε″ of permittivities of SiC increased firstly, and then decreased as the Al level increased in the region of 0-0.30eV and 0-1.0eV, respectively, covering the frequency range of 8.2-18GHz, of which SiC doped with Al_3-N complex had the greatest values.

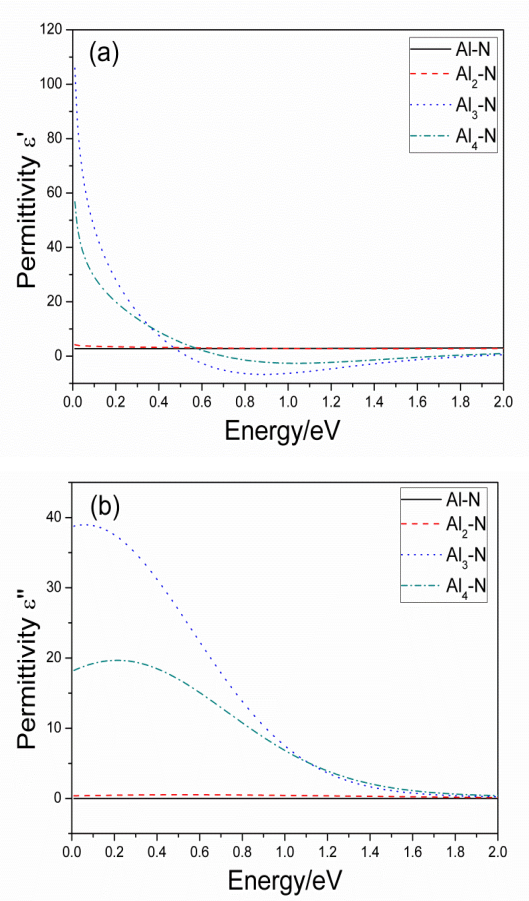

Fig. 4. Real part ε′ (a) and imaginary part ε″ (b) of permittivities of co-doped 3C-SiC as a function of energy

The imaginary part ε″ of permittivity of SiC represents the ability to dissipate incident electromagnetic wave, and the greater ε″ indicates the better microwave loss. The incorporation of Al into SiC crystal structure formed Al_{Si} point defects due to the substitution of Al atoms on Si atoms, and there would exist bound holes around these defects which would lead to electric conductance and electron relaxation losses under alternating electromagnetic field and cause the increase in ε″ [17]. In this study, when Al and N was doped as the same ratio, the hole from Al_{Si} defect was annihilated by the electron from N_C defect due to the substitution of N atom on C atom, resulting in the lowest ε′ and ε″ for all the co-doped SiC, in agreement with experimental results [14]. Results in Fig.3 showed that in the case of the same doping level of N atom, more Al doping increased the DOS near Fermi level as well the density of the carrier. This contributes to the increase of electric conductance and electron relaxation loss of SiC, which will lead to the increase in ε′ and ε″ in the whole. But more Al incorporating into SiC crystal structure also causes the increase of band gap of SiC and results in the decrease of intrinsic electric conductance of electron and hole carriers. In this sense, the increase of band gap will cause the decrease in ε′ and ε″ of SiC to some extent. Hence, for SiC doped with Al_4-N complex, the decrease of ε′ and ε″ was due to its broader band gap compared to the SiC doped with Al_3-N complex. Obviously, for SiC doped with Al_3-N complex, the more hole carriers from Al doping were dominant on the contribution of the greater values in ε′ and ε″ shown in Fig.4 under the interaction between hole concentration and band gap.

4. Conclusions

The defect formation energy, electronic structure and permittivities of 3C-SiC with different Al and N codoping levels were investigated by the first principles plane wave pseudo-potential method. It was found that the incorporation of N into SiC crystal structure lowered the formation energy of Al-doped SiC, with the minimum value of -1.423eV in the case of the same doping ratio of Al to N, and that the band gap of co-doped SiC increased with the increasing Al level. In the frequency range of 8.2-18GHz, both the real part ε′ and imaginary part ε″ of permittivities for co-doped 3C-SiC increased firstly, and then decreased with the increasing Al level. The SiC doped with Al_3-N complex showed the greatest values in ε′ and ε″. The results in this study will provide theoretical support for the adjustment of dielectric properties of SiC applied to microwave absorbers.

Acknowledgements

Authors would like to acknowledge the financial support of the Fund of the State Key Laboratory of Solidification Processing in NWPU (No. SKLSP201313).

References

[1] H. Bayrakdar, J. Magn. Magn. Mater. **323**, 1882 (2011).
[2] X. Huang, J. Chen, J. Zhang, L. Wang, Q. Zhang, J. Alloys Compd. **506**, 347 (2010).
[3] J. P. Calame, D. K. Abe, B. Levush, D. Lobas, J. Am. Ceram. Soc. **88**, 2133 (2005).
[4] S. Hayun, V. Paris, R. Mitrani, S. Kalabukhov, M. P. Dariel, E. Zaretsky, N. Frage, Ceram. Int. **38**, 6335 (2012).
[5] J. Yi, W. J. Xue, Z. P. Xie, W. Liu, L. X. Cheng, J. Chen, H. Cheng, Y. X. Gao, Mater. Sci. Eng. A **569**, 13 (2013).
[6] D. Li, H. B. Jin, M. S. Cao, T. Chen, Y. K. Dou, B. Wen, S. Agathopoulos, J. Am. Ceram. Soc. **94**, 1523 (2011).
[7] Z. Li, W. Zhou, F. Luo, Y. Huang, G. Li, X. Su, Mater. Sci. Eng. B **176**, 942 (2011).
[8] T. Yamamota, H. K. Yashida, Jpn. J. Appl. Phys. **38**, L166 (1999).

[9] R. Q. Wu, L. Shen, M. Yang, Z. D. Sha, Y. Q. Cai, Y. P. Feng, Phys. Rev. B **77**, 073203 (2008).
[10] A. Wu, Q. Song, Y. Li, Q. Hao, Comput. Theor. Chem. **977**, 92 (2011).
[11] Z. Wang, S. Xue, J. Li, F. Gao, J. Nanopart Res. **13**, 2887 (2011).
[12] Y. Dou, H. Jin, M. Cao, X. Fang, Z. Hou, D. Li, S. Agathopoulos, J. Alloys Compd. **509**, 6117 (2011).
[13] J. P. Perdew, K. Burke, M. Ernzerhof, Phys. Rev. Lett. **77**, 3865 (1996).
[14] X. Su, W. Zhou, J. Xu, J. Wang, X. He, C. Fu, Z. Li, J. Am. Ceram. Soc. **95**, 1388 (2012).
[15] Q. Hou, J. Li, C. Zhao, C. Ying, Y. Zhang, Physica B **406**, 1956 (2011).
[16] L. N. Chen, F. P. OuYang, S. S. Ma, X. Z. Wu, J. Xiao, H. Xu, Phys. Lett. A **374**, 4343 (2010).
[17] Z. Li, W. Zhou, X. Su, Y. Huang, G. Li, Y. Wang, J. Am. Ceram. Soc. **92**, 2116 (2009).

*Corresponding author: lizhmin@163.com